Complex Tetralogy of Fallot in an Acyanotic Adult Dog

Elizabeth L. Malcolm, DVM, and Ashley B. Saunders, DVM, DACVIM (Cardiology), *College Station, Texas*

INTRODUCTION

Differentiation of more complicated forms of tetralogy of Fallot (TOF), including pulmonary atresia with ventricular septal defect (VSD), from truncus arteriosus and other complex congenital malformations can be challenging with transthoracic echocardiography (TTE) alone, and though there are identifiable characteristics that can help make the differentiation, advanced imaging is typically required to provide a full picture of the anatomy and identify the sources of pulmonary blood flow. These defects have rarely been reported in the dog, cat, alpaca, and cow.[1-5] We describe the use of multimodality imaging with TTE, cardiac computed tomographic angiography (CTA), and augmented reality to diagnose TOF with pulmonary artery (PA) hypoplasia, absent left PA and multiple sources of collateral circulation contributing to pulmonary blood flow in an acyanotic adult dog.

CASE PRESENTATION

A 2-year-old adult male Shepherd mix weighing 22 kg was presented for further characterization of complex congenital heart disease (CHD). The owner originally reported moderate exercise intolerance and cyanosis that developed with excessive activity. A veterinary cardiologist performed TTE, which revealed a single large great artery arising from both ventricles, a VSD, and right ventricular (RV) enlargement. Propranolol 10 mg orally every 8 hours (0.47 mg/kg) was initiated. Exercise intolerance and cyanosis with activity resolved per the owner shortly after starting propranolol. Upon further evaluation at the Veterinary Medical Teaching Hospital, the dog's mucous membranes were pink, and grade III/VI right basilar systolic and II/VI diastolic murmurs were auscultated. The dog had a normal heart rate and regular rhythm with strong and synchronous femoral pulses. The remainder of the physical examination was unremarkable. The dog was administered a light sedative, and TTE was performed. Two-dimensional images obtained from the right parasternal long-axis view showed hypertrophy of the right ventricle (Figure 1, Video 1). Measurements included thickened RV free wall diameter in diastole of 9.1 mm (indexed, 0.42 cm/kg$^{0.25}$; abnormal range, >0.39 cm/kg$^{0.25}$), normal RV internal dimension in diastole of 2.51 cm (indexed, 0.91 cm/kg$^{0.33}$; abnormal range, >0.94 cm/kg$^{0.33}$), and normal tricuspid annular plane systolic excursion of 16.8 mm (indexed, 6.7 mm/kg$^{0.297}$; abnormal range, <4.8 mm/kg$^{0.297}$).[6] Additionally, there was mild right atrial dilation with anomalous vessels identified on the external surface of the left atrium and near the left atrioventricular groove (Figure 2, Video 2). A large great artery, expected to be the aorta, was identified overriding the interventricular septum with a VSD that measured approximately 3.4 mm from the aortic valve (Video 3). Color flow Doppler documented bidirectional VSD flow and aortic valve regurgitation directed entirely into the right ventricle (Figure 1). In the right parasternal short-axis view, a hypoplastic pulmonary valve (PV) was documented, with an estimated ratio of diameter at the PV (11.3 mm) to aortic diameter (29.6 mm) of 0.38 (abnormal range, <0.80; Figure 1, Video 4).[1] Spectral Doppler profiles had normal peak velocity (1.5 m/sec); however, the outflow tract and PA could not be properly demonstrated to obtain optimal cursor alignment. Branch PAs could not be located with TTE. A single left coronary artery was suspected (Figure 1). A patent ductus arteriosus was not present. These findings were most consistent with a tentative diagnosis of TOF with hypoplasia or atresia of the PAs and the presence of collateral vessels. Packed cell volume (54%; reference range, 37%-55%) and total solids (7.0 g/dL; reference range, 6.0-8.0 g/dL) were normal.[7] Pulse oximetry was 98%. Advanced imaging was recommended to fully evaluate the anatomy. Two weeks later, the dog was induced under general anesthesia, and CTA was performed to establish a diagnosis, characterize the PAs, and evaluate pulmonary blood flow. The scan was performed under breath hold with tube current of 250 mA, tube voltage of 120 kV, 0.9 pitch, a scan width of 0.6 mm, and reconstructed with an overlap of 3 mm. Contrast-enhanced CTA was performed with 47 mL nonionic contrast medium (300 mg I/mL) administered through a peripheral intravenous catheter in the left cephalic vein using a power injector. Postcontrast scans were gated to 80 Hounsfield units on the cranial vena cava in immediate succession. Transverse plane images were reconstructed with a soft tissue algorithm. In reconstructed images (Figure 3), the PV was hypoplastic, and a contiguous main PA was identified with a hypoplastic right branch PA perfusing the right cranial lung field and an absent left branch PA. A single left coronary artery was confirmed. The CTA study was further evaluated by importing the Digital Imaging and Communications in Medicine images into a three-dimensional viewing software platform that displays a reconstructed model as a stereoscopic object viewed with three-dimensional glasses. In the multiplanar reconstructed model, multiple major aortopulmonary collateral arteries (MAPCAs) were identified arising from the descending aorta in addition to an enlarged vessel on the right side in the region of the expected bronchoesophageal artery that tapered into numerous small, tortuous collateral vessels (Figure 4). Additionally, there were two large anastomosing collateral arteries that coursed over bronchi to perfuse the caudolateral lung fields on both sides of the thorax. Numerous tortuous vessels were also identified along the left side of the heart, in the mediastinum, and on the diaphragm (Figure 2). The findings on CTA facilitated confirmation of a diagnosis

From the Department of Small Animal Clinical Sciences, College of Veterinary Medicine and Biomedical Sciences, Texas A&M University, College Station, Texas.

Keywords: Augmented reality, Canine, Computed tomographic angiography, Major aortopulmonary collateral arteries

Correspondence: Ashley B. Saunders, DVM, DACVIM (Cardiology), Department of Small Animal Clinical Sciences, College of Veterinary Medicine and Biomedical Sciences, Texas A&M University, College Station, TX 77843-4474. (E-mail: *asaunders@tamu.edu*).

2468-6441/$36.00

https://doi.org/10.1016/j.case.2023.12.010

VIDEO HIGHLIGHTS

Video 1: Two-dimensional TTE, right parasternal long-axis view, demonstrates right ventricular (RV) hypertrophy and collateral vessels near the left atrium and atrioventricular groove.
Video 2: Two-dimensional TTE with color flow Doppler, right parasternal long-axis view, demonstratesg color flow in collateral vessels near the left atrium and atrioventricular groove.
Video 3: Two-dimensional TTE with color flow Doppler, right parasternal long-axis view, demonstrates the aorta overriding the ventricular septum and left-to-right flow into the right ventricle with color flow Doppler.
Video 4: Two-dimensional TTE with color flow Doppler, right parasternal short-axis view, demonstrates left-to-right flow into the right ventricle and the hypoplastic PV.

View the video content online at www.cvcasejournal.com.

of TOF with PA hypoplasia, absent left branch PA, and multiple sources of pulmonary circulation, including MAPCAs, a dilated bronchoesophageal artery, and numerous acquired collateral vessels. The dog was continued on propanol with routine recheck evaluations scheduled and has continued to do well at home 3 months later.

DISCUSSION

TOF is a complex form of CHD with abnormal position of the infundibular septum and malalignment resulting in VSD, overriding of the aorta, hypertrophy of the right ventricle, and pulmonary stenosis in which hypoplasia can occur at the level of the RV outflow tract, PV, or PAs.[8] PA hypoplasia has been reported in approximately 33% of dogs (five of 15).[1] In the dog reported here, a hypoplastic PV was identified on TTE, but the PAs could not be identified, and subsequently, PA hypoplasia with absent left branch PA was diagnosed on CTA. The utility of CTA includes documentation of the PAs as native, contiguous, atretic, or absent, as well as characterization of the pulmonary circulation and coronary anomalies.[9] With CTA, detailed information regarding collateral vessels specifically related to number, size, origin, and connections to other vessels can be fully characterized.[9] Sources of pulmonary perfusion may include native PAs, patent ductus arteriosus, MAPCAs, bronchial arteries, and acquired collateral vessels.[9,10] In humans, the predominant source of pulmonary blood supply in severe forms of TOF is a patent ductus arteriosus or MAPCAs, and assessment of the origin and course of these and any other abnormal vessels is essential for clinical decision-making and preoperative planning.[8,9,11] The dog in this report was characterized as having type B pulmonary circulation, which includes native PA flow and MAPCAs compared with only native PAs (type A) or MAPCAs (type C).[12] The presence of MAPCAs is associated with PA hypoplasia or atresia.[10,12] Absence of the left branch PA in TOF is rare in humans and has been attributed to involution of the patent ductus arteriosus.[8] The spectrum of abnormalities with TOF can also include abnormal coronary artery origin and branching and is important to recognize before surgical planning.[8] Although the prevalence of coronary artery anomalies in humans with TOF is relatively low, close evaluation of coronary anatomy before surgical intervention is essential to minimize risk for coronary artery damage.[8] There is a paucity of information regarding the prevalence of coronary artery anomalies in dogs with TOF, likely resulting from infrequent use of advanced imaging and uncommonly performed surgical intervention in this species. Cyanosis is

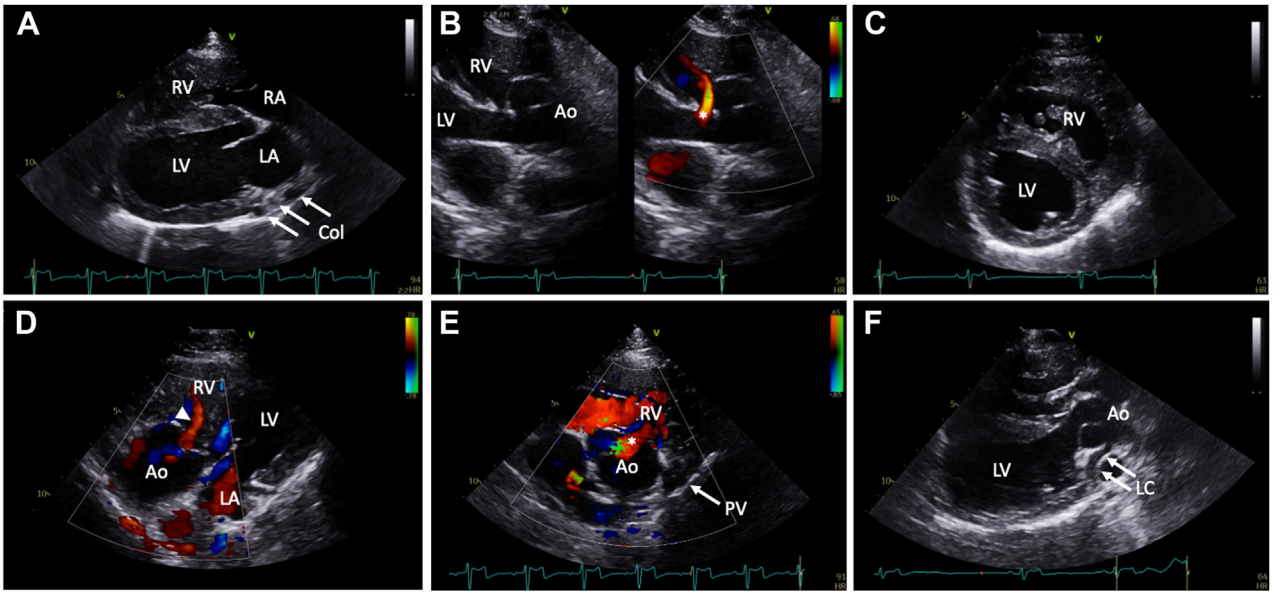

Figure 1 Two-dimensional TTE in a dog. **(A)** Right parasternal long-axis four-chamber view demonstrates collateral vessels (Col) near the left atrium (LA) and atrioventricular groove, **(B)** right parasternal long-axis view demonstrates the aorta (Ao) overriding the ventricular septum and left-to-right flow with color flow Doppler (*asterisk*), **(C)** right parasternal short-axis view at the level of the ventricles demonstrates right ventricular enlargement, **(D)** left parasternal long-axis view with color flow Doppler demonstrates aortic valve regurgitation (*arrowhead*) directed preferentially into the right ventricle (RV), **(E)** right parasternal short-axis view at the base of the heart with color flow Doppler demonstrates left-to-right flow (*asterisk*) into the RV and PV hypoplasia, and **(F)** right parasternal oblique long-axis view demonstrates the single left coronary artery (LC). *LV*, Left ventricle; *RA*, right atrium.

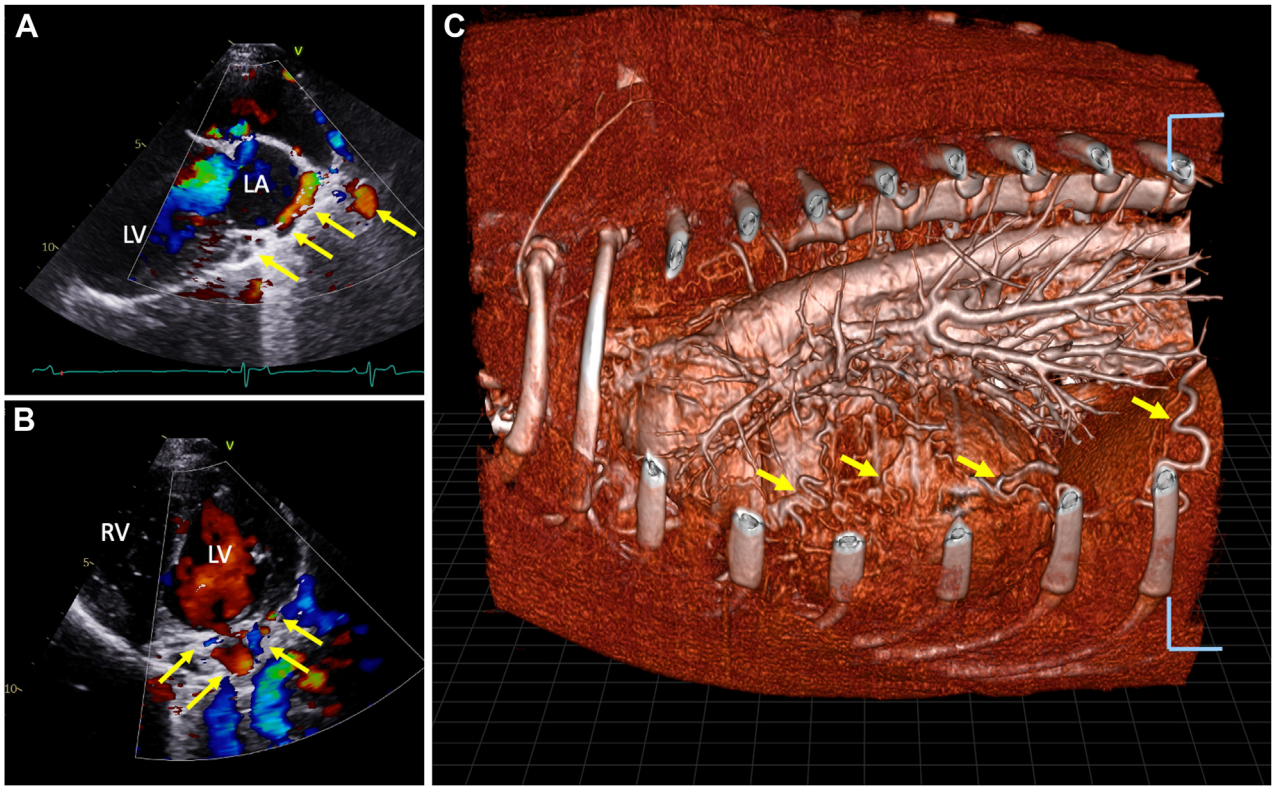

Figure 2 Two-dimensional TTE with color flow Doppler right parasternal **(A)** and left parasternal **(B)** views obliqued to demonstrate the collateral vessels along the left side of the heart (*arrows*). Multiplanar CTA reconstruction viewed in a three-dimensional software platform demonstrates multiple acquired collateral vessels (*arrows*) in a surface-rendered model displaying the left side of the thorax **(C)**.

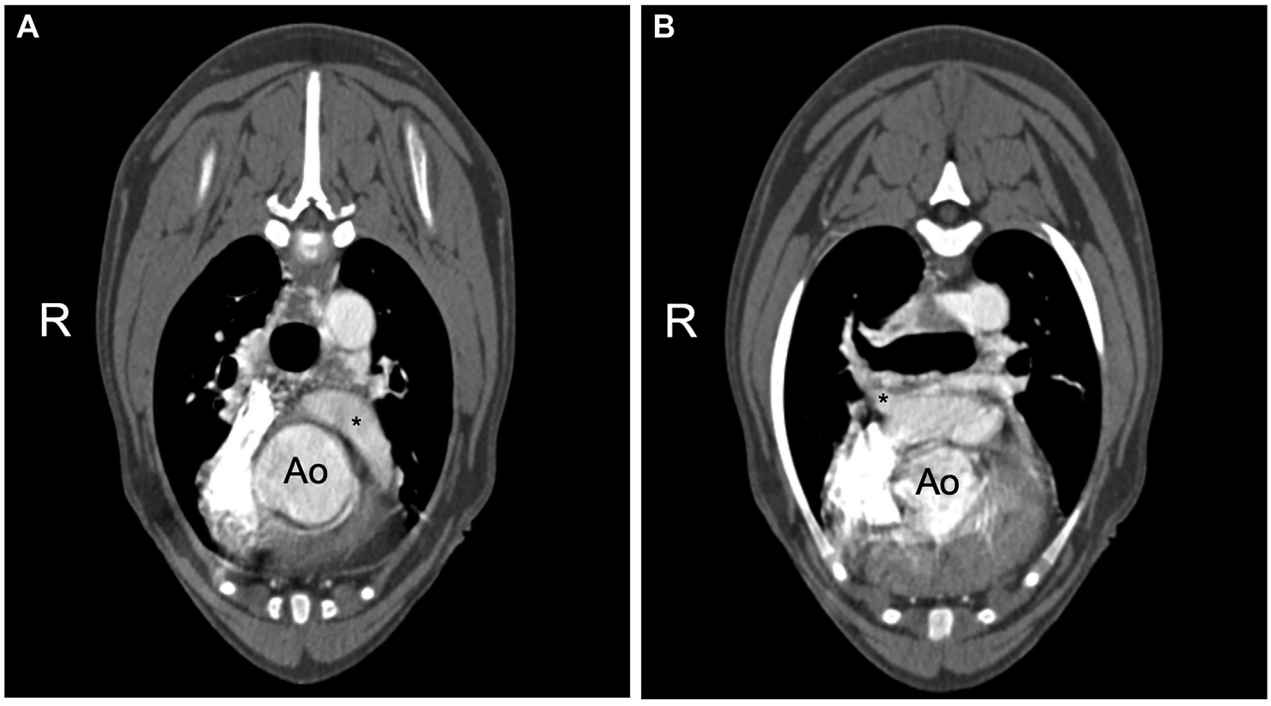

Figure 3 CTA reconstruction in a transverse view demonstrates **(A)** PA hypoplasia (*asterisk*) and **(B)** the hypoplastic right branch PA directed cranially (*asterisk*). *Ao*, Aorta.

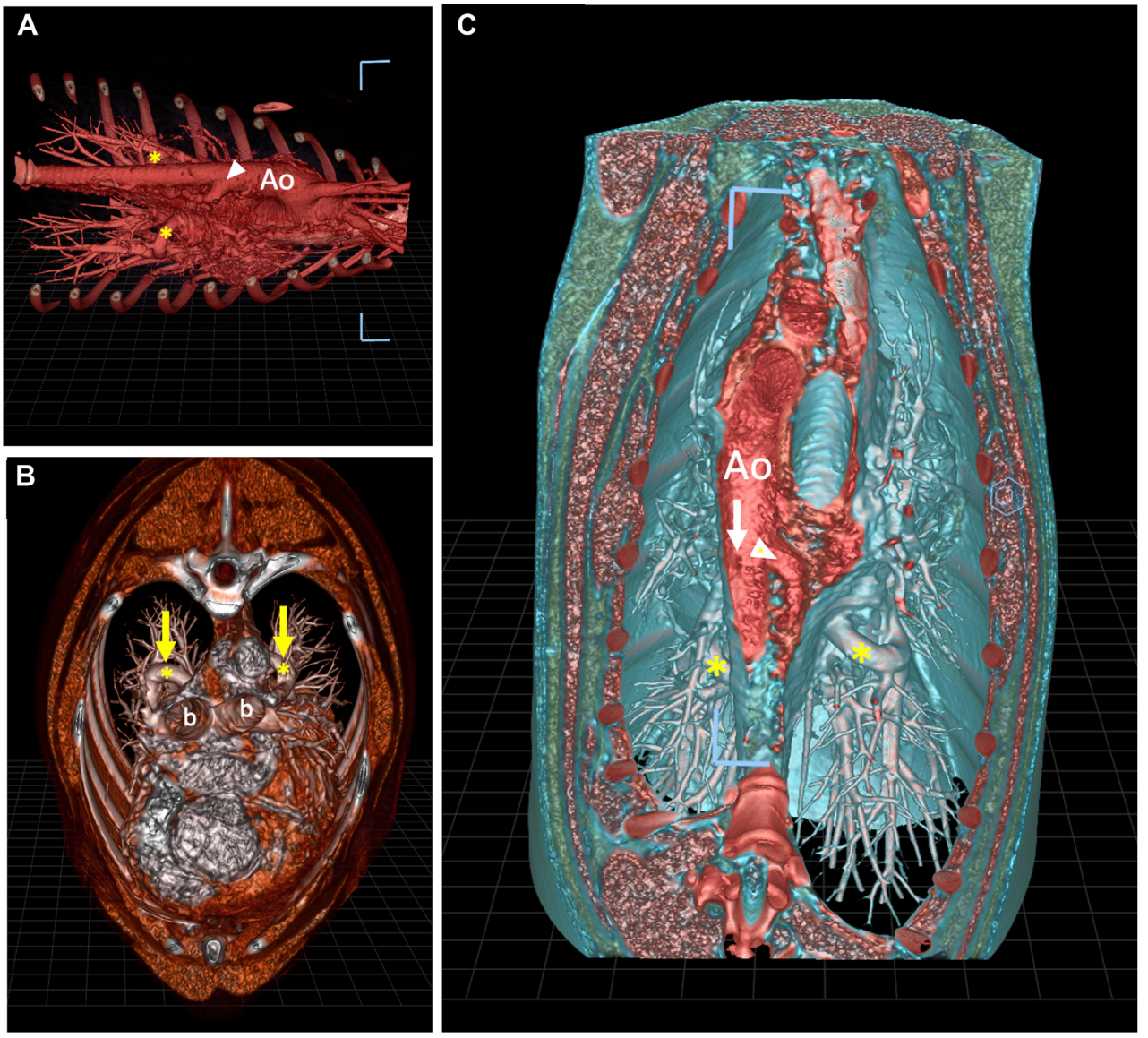

Figure 4 CTA reconstructions viewed in a three-dimensional software platform demonstrate **(A)** from a dorsal obliqued view (head to the right), the enlarged bronchoesophageal artery originating from the aorta (Ao) at the fifth to sixth intercostal space on the right (*arrowhead*) and two large anastomosing collateral vessels (*asterisk*) in a volume-rendered model, **(B)** from a transverse view, the peripheral collateral pulmonary vessels (*asterisk with arrow*) in close proximity to the bronchi (b) in a surface and volume-rendered model, and **(C)** from a dorsal view (head at the top), cutting into the lumen of the Ao and enlarged bronchoesophageal artery (*arrowhead*) to demonstrate the origin of a MAPCA (*arrow*) in a surface- and volume-rendered model.

frequently but not always present in humans and animals with TOF.[1,8] Multiple sources of pulmonary blood flow and use of beta blockade were the most likely reasons for the lack of cyanosis and clinical signs in this dog.

Collateral vessels were identified on TTE in the dog reported here, similar to what is reported in children.[10] Although TTE is valuable for initial evaluation of complex CHD, advanced imaging techniques with selective angiography, CTA, and magnetic resonance angiography are essential for establishing the diagnosis and characterizing the source and extent of the pulmonary blood supply. Variations of TOF have been reported in dogs and cats, but detailed characterization of the pulmonary blood supply with multimodal imaging has not been consistently described. A case report of an adult dog diagnosed with pulmonary atresia and VSD identified MAPCAs on transesophageal echocardiography and angiography.[1] In another report, CTA was essential in the differentiation and diagnosis of pulmonary atresia and VSD with MAPCAs from truncus arteriosus in two young cats with similar TTE features of a single large great vessel overriding a large VSD with no visible pulmonary trunk.[3] Advancements in technology have created unique ways to assess complex CHD, including use of augmented and virtual reality systems that allow the operator to manipulate a three-dimensional model or hologram in 360° rotation that has been derived from a CTA data set. This type of imaging can increase diagnostic accuracy and improve clinical decision-

making.[10,13] Surgical options for TOF in veterinary patients have been limited but are possible, and management is typically directed toward palliation of clinical signs with a modified Blalock-Taussig shunt or definitive repair in dogs but can be limited by surgical center availability and cost.[14,15] Humans with adequate collateral pulmonary perfusion can survive into adulthood without surgical intervention,[10] similar to the dog in this report.

CONCLUSION

The case presented here describes TOF with pulmonary hypoplasia and absent left branch PA in an acyanotic adult dog with pulmonary perfusion through a combination of MAPCAs, a large bronchoesophageal artery, and acquired collateral vessels that was diagnosed using a combination of TTE, cardiac CTA, and augmented reality.

ETHICS STATEMENT

The authors declare that the work described has been carried out in accordance with the ARRIVE guidelines and with the U.K. Animals (Scientific Procedures) Act, 1986 and associated guidelines, EU Directive 2010/63/EU for animal experiments, or the National Research Council's Guide for the Care and Use of Laboratory Animals.

CONSENT STATEMENT

Complete written informed consent was obtained from the patient (or appropriate parent, guardian, or power of attorney) for the publication of this study and accompanying images.

FUNDING STATEMENT

The authors declare that this report did not receive any specific grant from funding agencies in the public, commercial, or not-for-profit sectors.

DISCLOSURE STATEMENT

The authors report no conflict of interest.

ACKNOWLEDGMENTS

We thank Julia Lindholm, DVM, DACVIM (Cardiology) for case referral, Dianna Ovbey, DVM, MS, DACVAA for anesthesia support, and Hollye Felps, LVT, Gwendolyn Levine, DVM, DACVP, DACVR, DACVR-EDI, and Jillian Myers, DVM for CTA imaging support.

SUPPLEMENTARY DATA

Supplementary data to this article can be found online at https://doi.org/10.1016/j.case.2023.12.010.

REFERENCES

1. Chetboul V, Pitsch I, Tissier R, Gouni V, Misbach C, Trehiou-Sechi E, et al. Epidemiological, clinical, and echocardiographic features and survival times of dogs and cats with tetralogy of Fallot: 31 cases (2003–2014). J Am Vet Med Assoc 2016;249:909-17.
2. Tou SP, Keene BW, Barker PC. Pulmonary atresia and ventricular septal defect with aortopulmonary collaterals in an adult dog. J Vet Cardiol 2011;13:271-5.
3. Markovic LE, Scansen BA, Potter BM. Role of computed tomography angiography in the differentiation of feline truncus arteriosus communis from pulmonary atresia with ventricular septal defect. J Vet Cardiol 2017;19:514-22.
4. Stieger-Vanegas SM, Scollan KF, Meadows L, Sisson D, Schlipf J, Riebold T, et al. Cardiac-gated computed tomography angiography in three alpacas with complex congenital heart disease. J Vet Cardiol 2016;18:88-98.
5. Nakade T, Uchida Y, Otomo K. Three cases of bovine extreme tetralogy of Fallot. J Vet Med Sci 1993;55:161-7.
6. Visser LC, Nishimura S, Oldach MS, Belanger C, Gunther-Harrington CT. Echocardiographic assessment of right heart size and function in dogs with pulmonary valve stenosis. J Vet Cardiol 2019;26:19-28.
7. Tvedten HW. Hematology of the normal dog and cat. Vet Clin North Am Small Anim Pract 1981;11:209-17.
8. Jacobs ML. Congenital heart Surgery Nomenclature and Database Project: tetralogy of Fallot. Ann Thorac Surg 2000;69(4 Suppl):S77-82.
9. Zucker EJ. Computed tomography in tetralogy of Fallot: pre- and postoperative imaging evaluation. Pediatr Radiol 2022;52:2485-97.
10. Alex A, Ayyappan A, Valakkada J, Kramadhari H, Sasikumar D, Menon S. Major aortopulmonary collateral arteries. Radiol Cardiothorac Imaging 2022;4:e210157.
11. Petit CJ, Glatz AC, Goldstone AB, Law MA, Romano JC, Maskatia SA, et al. Pulmonary hypoplasia in neonates with tetralogy of Fallot. J Am Coll Cardiol 2023;82:615-27.
12. Tchervenkov CI, Roy N. Congenital heart Surgery Nomenclature and Database Project: pulmonary atresia-ventricular septal defect. Ann Thorac Surg 2000;69:S97-105.
13. Silva JNA, Southworth M, Raptis C, Silva J. Emerging applications of virtual reality in cardiovascular medicine. J Am Coll Cardiol Basic Transl Sci 2018;3:420-30.
14. Orton EC, Mama K, Hellyer P, Hackett TB. Open surgical repair of tetralogy of Fallot in dogs. J Am Vet Med Assoc 2001;219:1089-93.
15. Brockman DJ, Holt DE, Gaynor JW, Theman TE. Long-term palliation of tetralogy of Fallot in dogs by use of a modified Blalock-Taussig shunt. J Am Vet Med Assoc 2007;231:721-6.